The *deltaA* gene of zebrafish mediates lateral inhibition of hair cells in the inner ear and is regulated by *pax2.1*

Bruce B. Riley*, Ming-Yung Chiang, Lisa Farmer and Rebecca Heck

Biology Department, Texas A&M University, College Station, TX 77843-3258, USA

*Author of correspondence (e-mail: briley@mail.bio.tamu.edu)

SUMMARY

Recent studies of inner ear development suggest that hair cells and support cells arise within a common equivalence group by cell-cell interactions mediated by Delta and Notch proteins. We have extended these studies by analyzing the effects of a mutant allele of the zebrafish *deltaA* gene, *deltaA^{dx2}*, which encodes a dominant-negative protein. *deltaA$^{dx2/dx2}$* homozygous mutants develop with a 5- to 6-fold excess of hair cells and a severe deficiency of support cells. In addition, *deltaA$^{dx2/dx2}$* mutants show an increased number of cells expressing *pax2.1* in regions where hair cells are normally produced. Immunohistological analysis of wild-type and *deltaA$^{dx2/dx2}$* mutant embryos confirmed that *pax2.1* is expressed during the initial stages of hair cell differentiation and is later maintained at high levels in mature hair cells. In contrast, *pax2.1* is not expressed in support cells. To address the function of *pax2.1*, we analyzed hair cell differentiation in *no isthmus* mutant embryos, which are deficient for *pax2.1* function. *no isthmus* mutant embryos develop with approximately twice the normal number of hair cells. This neurogenic defect correlates with reduced levels of expression of *deltaA* and *deltaD* in the hair cells in *no isthmus* mutants. Analysis of *deltaA$^{dx2/dx2}$; no isthmus* double mutants showed that *no isthmus* suppresses the *deltaA^{dx2}* phenotype, probably by reducing levels of the dominant-negative mutant protein. This interpretation was supported by analysis of *T(msxB)^{b220}*, a deletion that removes the *deltaA* locus. Reducing the dose of *deltaA^{dx2}* by generating *deltaA^{dx2}/T(msxB)^{b220}* *trans*-heterozygotes weakens the neurogenic effects of *deltaA^{dx2}*, whereas *T(msxB)^{b220}* enhances the neurogenic defects of *no isthmus*. *mind bomb*, another strong neurogenic mutation that may disrupt reception of Delta signals, causes a 10-fold increase in hair cell production and is epistatic to both *no isthmus* and *deltaA^{dx2}*. These data indicate that *deltaA* expressed by hair cells normally prevents adjacent cells from adopting the same cell fate, and that *pax2.1* is required for normal levels of Delta-mediated lateral inhibition.

Key words: *deltaA*, *pax2.1*, Inner ear, Hair cell, Support cell, Lateral inhibition, Zebrafish

INTRODUCTION

The inner ear consists of a complex series of chambers, each containing a specialized epithelium composed of sensory hair cells interspersed with support cells (Anniko, 1983; Lewis et al., 1985). Hair cells bear ciliary bundles that project into the lumen of the ear. Lateral displacement of the ciliary bundles due to sound vibrations or accelerational forces stimulates the hair cells to transmit neural signals associated with hearing or detection of motion and orientation. The role of support cells is less certain, but they appear to provide factors in trans required for normal hair cell function and survival (Riley and Grunwald, 1996; Riley et al., 1997; Haddon et al., 1998a), a role analogous to that of glial cells in the central nervous system. In addition, support cells can act as stem cells that divide asymmetrically to give rise to additional support cells and new hair cells (Corwin and Warchol, 1991; Presson et al., 1996). The latter function provides a mechanism for hair cell regeneration in adult tissues, but it remains to be established whether a similar process operates during embryonic development.

The first sensory epithelia to develop in the otic vesicle are the maculae, which are associated with dense crystalline otoliths that assist hair cells in sensing sound and linear acceleration (Haddon and Lewis, 1996). Subsequently, sensory epithelia called cristae develop in the semicircular canals, which primarily sense angular acceleration. Unlike maculae, cristae are not associated with otoliths.

Genetic studies in mouse and zebrafish have revealed a number of mutations affecting various stages of otic development, including induction of the otic placode, morphogenesis of the otic vesicle, and differentiation and function of sensory hair cells (Epstein et al., 1991; Lufkin et al., 1991; Chisaka et al, 1992; Mansour et al., 1993; Cordes and Barsh, 1994; Erkman et al., 1996; Torres et al., 1996; Xiang et al., 1997; Hadrys et al., 1998; Mendonsa and Riley, 1999; Moens et al., 1998; Self et al., 1998; Wang et al., 1998; Bermingham et al., 1999). Nevertheless, the mechanisms

controlling the initial stages of hair cell and support cell differentiation remain largely unknown.

The alternating pattern of hair cells and support cells has led to the suggestion that their differentiation is coordinately regulated by interactions between Delta, a tethered ligand, and Notch, its receptor, in a process known as lateral inhibition or lateral specification (Campos-Ortega, 1994; Artavanis-Tsakonas et al., 1995; Lewis, 1996). This process forces neighboring cells belonging to the same equivalence group to adopt different cell fates. Typically, all cells in an equivalence group initially express low levels of both Delta and Notch, which later become mutually antagonistic. The balance in expression of these genes is disrupted when inductive signals or stochastic effects stimulate a subset of cells in the equivalence group to differentiate as the 'default' cell type and express high levels of Delta. Elevated Delta signaling from the default cell type increases activity of Notch receptors on neighboring cells, causing the latter to downregulate Delta expression and adopt an alternative cell fate. Thus, lateral inhibition provides a general mechanism of short-range signaling that produces 'salt and pepper' patterns of distinct cell types that differentiate in close proximity to one another. Mutations that disrupt the function of *Delta* or *Notch* result in overproduction of the default cell type. For example, in a wide range of animal species, disruption of Delta-Notch signaling causes 'neurogenic' phenotypes characterized by overproduction of early neural cell types at the expense of alternative cell types (Artavanis-Tsakonas et al., 1995; Chitnis et al., 1995; de la Pompa et al., 1997; Appel and Eisen, 1998; Haddon et al., 1998b). The hypothesis that hair cells and support cells are regulated by lateral inhibition is supported by recent findings in chick and zebrafish that differentiating hair cells, but not support cells, express high levels of multiple *delta* homologs (Adam et al., 1998; Haddon et al., 1998a). Furthermore, zebrafish embryos homozygous for the *mind bomb* (*mib*) mutation produce a large excess of hair cells but virtually no support cells. Although the *mib* gene has not been identified, the mutation is believed to impair Delta-Notch signaling because *mib−* mutants show a dramatic neurogenic phenotype that affects virtually the entire nervous system (Jiang et al, 1996; Schier et al., 1996).

To directly assess the role of endogenous Delta proteins, we have analyzed a mutation affecting the *deltaA* (*dlA*) gene of zebrafish. The mutant allele, dlA^{dx2}, is weakly dominant and incompletely penetrant. In homozygous mutants, penetrance is more complete and the phenotype is much more severe. The mutation results from a mis-sense mutation in which a highly conserved cysteine residue in EGF-repeat 2 is replaced by tyrosine. The resulting mutant protein exhibits dominant-negative activity, causing a more severe neurogenic phenotype than a null mutation of *dlA* (Appel et al., 1998).

Here, we show that $dlA^{dx2/dx2}$ homozygotes develop with a large excess of hair cells and display a notable expansion in the number of cells expressing *pax2.1* in the vicinity of the sensory epithelia. More detailed analysis confirmed that *pax2.1* is a reliable marker of hair cell differentiation. Support cells, which do not express *pax2.1*, are grossly deficient in $dlA^{dx2/dx2}$ mutant embryos. $noi^{tb21/tb21}$ mutants, which are disrupted for *pax2.1* function (Brand et al., 1996; Pfeffer et al., 1998), also produce a weak neurogenic phenotype that appears to result from reduced expression of *dlA* and *dlD*. In contrast,

noi^{tb21} partially suppresses the dlA^{dx2} phenotype by reducing expression of the dominant-negative dlA^{dx2} protein. Together, these data indicate that *dlA* normally restricts the number of hair cells that differentiate in the inner ear, and *pax2.1* is required for normal levels of *dlA*-mediated lateral inhibition.

MATERIALS AND METHODS

Strains
The wild-type line was obtained by hybridizing the AB line (Eugene, OR) to a partially inbred line of genetically similar store-bought fish. The dlA^{dx2} mutation was induced in the wild-type background with ethylnitrosourea (Appel et al., 1999). The $T(msxB)^{b220}$ mutation was induced in the AB line with gamma rays (Fritz et al., 1996). The noi^{tb21} and mib^{ta52b} mutations were induced with ENU in the Tu wild-type strain (Brand et al., 1996; Jiang et al., 1996).

Developmental conditions and identification of mutant embryos
Embryos were developed in an incubator at 28.5°C. Developmental stages are expressed in terms of h (hours of development). $dlA^{dx2/dx2}$ homozygotes were identified at 24 h by several criteria: the floor plate of the neural tube is partially disrupted, the main body axis usually shows strong dorsal curvature, and the hindbrain and otic vesicles often show severe morphogenetic defects. The majority of $dlA^{dx2/+}$ heterozygotes show none of these defects at 24 h, although 1-5% show mild dorsal curvature. To identify $dlA^{dx2/+}$ heterozygotes, hair cells were visualized in live embryos at 22-24 h. Wild-type embryos invariably show two utricular hair cells during this period, whereas $dlA^{dx2/+}$ embryos usually show three to five utricular hair cells by 24 h. $dlA^{dx2}/T(msxB)^{b220}$ *trans*-heterozygotes resemble $dlA^{dx2/dx2}$ homozygotes but are usually less severely affected. $noi^{tb21/tb21}$ homozygotes were identified at 24 h by disruption of the midbrain-hindbrain border (Brand et al, 1996). $dlA^{dx2/dx2}$; $noi^{tb21/tb21}$ double mutants resemble $noi^{tb21/tb21}$ single mutants, except that double mutants also show partial disruption of the floor plate. $mib^{ta52b/ta52b}$ homozygotes resemble $dlA^{dx2/dx2}$ homozygotes, but $mib^{ta52b/ta52b}$ mutants are usually more severely affected and show somite defects as well. $mib^{ta52b/ta52b}$; $noi^{tb21/tb21}$ double mutants resemble $mib^{ta52b/ta52b}$ single mutants, but double mutants also show disruption of the midbrain-hindbrain border.

In situ hybridization
Embryos were fixed in MEMFA (0.1 M MOPS at pH 7.4, 2 mM EGTA, 1 mM MgSO₄, 3.7% formaldehyde). In situ hybridizations (Stachel et al., 1993) were performed at 67°C using probes for *pax-2.1* (Krauss et al., 1991), *dlA* or *dlD* transcripts (Appel and Eisen, 1998; Haddon et al., 1998b).

Immunohistochemistry
Embryos were fixed in MEMFA and washed for 1-2 hours at room temperature with PBT.LS (0.8% sodium chloride, 0.02% potassium chloride, 0.02 M sodium phosphate, pH 7.3, 2 mg/ml bovine serum albumin, 10% lamb serum and 0.1% Triton X-100). Embryos older than 24 h were initially washed with PBT.LS containing higher concentrations of Triton X-100: 30 h embryos were washed with 0.5% Triton X-100, and 48 or 60 h embryos with 2.5% Triton X-100. In all subsequent washes and incubations, PBT.LS with 0.1% Triton X-100 was used. Embryos were incubated with a 1:100 dilution of primary antibody directed against mouse Pax2 (Berkeley Antibody Company) or acetylated tubulin (Sigma T-6793). Embryos were then washed and incubated with one or more of the following secondary antibodies: Cy3-conjugated sheep anti-mouse IgG (Sigma C-2181, diluted 1:50), Cy3-conjugated sheep anti-rabbit IgG (Sigma C-2306, diluted 1:50), Alexa 488-conjugated goat anti-mouse IgG (Molecular Probes # A-

11001, diluted 1:50), or HRP-conjugated goat anti-rabbit IgG (Sigma A-0545, diluted 1:200). For sectioning, embryos were embedded in Immunobed resin (Polysciences No. 17324) and cut into 4 μm sections.

RT-PCR

mRNA was extracted from groups of 40 embryos (24 h) or 30 embryos (30 h) dissolved in 800 μl Tri Reagent (Sigma no. T9424) according to manufacturer specifications. Reverse transcription was performed in 20 μl reactions using Superscript II (Gibco-BRL) with 2 μg total RNA and 2 pmole of the downstream dlA-specific primer (see below). 1 μl (5%) of the RT-PCR reaction product was then PCR amplified with Amplitaq (Perkin-Elmer) and 2 pmole each of dlA-specific primers using the following program: 105 seconds at 95°C; 21 cycles of 94°C for 45 seconds, 55°C for 55 seconds, 72°C for 45 seconds; and a final extension for 6 minutes at 72°C. Sequences for dlA-specific primers are: Upstream primer, TCAGAGTCAAGGTATTCCG. Downstream primer, TCAGTA-CAGAGAACCAGCTC.

RESULTS

Identification of *pax2.1* as a potential marker of hair cell differentiation

To analyze inner ear defects in *dlA^dx2^* mutant embryos, we examined expression of *pax2.1*, an early marker of otic placode and vesicle development. At 24 h, *pax2.1* transcripts are localized to the medial portion of the otic vesicle in both wild-type and *dlA^dx2/dx2^* mutant embryos, with increased expression levels seen in clusters of cells at the anterior and posterior limits of this expression domain (Fig. 1A-C). In *dlA^dx2/dx2^* embryos, the number of cells with elevated *pax2.1* expression is variably but consistently increased. These cells lie within the regions of the otic vesicle where sensory epithelia first develop, suggesting that the extra *pax2.1*-expressing cells in *dlA^dx2/dx2^* mutants might reflect overproduction of hair cells. Use of a polyclonal antibody directed against mouse Pax2 produces a pattern identical to the *pax2.1* expression pattern and reveals increased numbers of Pax2-expressing cells in the anterior and posterior ends of the otic vesicle in *dlA^dx2/dx2^* mutants (Fig. 1E,F). Co-staining with a second antibody directed against acetylated tubulin confirms that virtually all of the cells with elevated Pax2 staining are indeed hair cells.

Because two homologs of *pax2* have been identified in the zebrafish, *pax2.1* and *pax2.2* (Pfeffer et al., 1998), we wished to determine whether the mouse antibody recognizes both zebrafish proteins. Therefore, we examined the pattern of Pax2 antibody staining in *no isthmus* (*noi*) mutants, which are disrupted in *pax2.1* function. The allele studied here, *noi^tb21^*, produces a truncated protein lacking a significant portion of the carboxy terminus to which the antibody normally binds (Lun and Brand, 1998). Nevertheless, *noi^tb2/tb211^* mutants cannot be distinguished from wild-type embryos by anti-Pax2 staining at 14 h (not shown). However, *noi^tb2/tb211^* mutants show diminished staining in all *pax2.1*-expressing tissues by 18 h (Fig. 1F-I, and data not shown). Residual staining at 18 h does not simply reflect cross-reactivity to *pax2.2* since staining is similarly reduced in the pronephros, which does not express *pax2.2*. Moreover, Pax2 staining is undetectable in *noi^tb2/tb211^* mutants by 24 h (Fig. 1J and data not shown), even though expression of *pax2.2* is not diminished in *noi−* mutants (Pfeffer et al., 1998). These data suggest that the mouse Pax2 antibody primarily recognizes zebrafish *pax2.1* and that the reduced staining observed in *noi^tb2/tb211^* embryos results from failure to maintain normal levels of *pax2.1* expression (Brand et al., 1996).

Hair cells express *pax2.1* at all stages of differentiation in wild-type embryos

High level expression of *pax2.1* in differentiating hair cells has not been previously reported, so we examined this correlation in more detail at various stages of inner ear development. *pax2.1* is expressed uniformly in cells throughout the medial half of the nascent otic vesicle at 18.5 h (Fig. 1G) but dramatically upregulates in hair cells by 24 h (Fig. 1D). At 30 h, the number of cells in the developing maculae that express high levels of *pax2.1* increases roughly two-fold from that seen at 24 h (Fig. 2A), which agrees with the observed increase in the number of hair cells (Haddon and Lewis, 1996; Riley et al., 1997). In contrast, *pax2.1* expression begins to downregulate in cells surrounding the presumptive hair cells. Sectioning of embryos stained with anti-Pax2 and anti-acetylated tubulin confirmed that all hair cells express high levels of *pax2.1* whereas support cells express little or none (Fig. 2B). By 48 h, additional cells expressing high levels of *pax2.1* accumulate in maculae, reflecting comparable changes in the number and distribution of hair cells. Maculae are also surrounded by rings of cells expressing *pax2.1* at lower levels (Fig. 2C). This lower expression probably marks nascent hair cells at the margins of the maculae, as it presages the future dimensions of macular growth. Sections of 60 h embryos confirm that all macular hair cells continue to express high levels of *pax2.1* (Fig. 2D). Although support cells do not express detectable levels of *pax2.1*, the margins of maculae often contain isolated cells that fully span the epithelium and also express low levels of *pax2.1*. The identity of these cells is uncertain but they probably correspond to nascent hair cells, which develop from cells that superficially resemble support cells (Haddon et al., 1998a). Cristae, which are the sensory patches associated with the semicircular canals, begin to develop at 60 h, and individual cells within the cristae also express *pax2.1* (Fig. 2E). Analysis of specimens double stained for *pax2.1* and acetylated tubulin confirms that these, too, are hair cells, and that support cells in the developing cristae do not express *pax2.1* (Fig. 2F). Thus, *pax2.1* appears to be induced during early stages of hair cell differentiation and is later maintained at high levels in mature hair cells. In contrast, support cell do not express detectable levels of *pax2.1*.

Hair cell differentiation in *dlA^dx2/dx2^* mutant embryos

In *dlA^dx2/dx2^* mutants at 30 h, presumptive hair cells expressing high levels of *pax2.1* become so numerous that the anterior and posterior maculae often become contiguous (Fig. 3A). Sections of *dlA^dx2/dx2^* embryos reveal that these expanded maculae develop with a gross excess of hair cells, all of which express high levels of *pax2.1* (Fig. 3C). Support cells, on the contrary, are almost totally missing. The imbalance in the ratio of hair cells to support cells severely distorts the shape of the maculae and alters the morphology of the otic vesicle (Fig. 3C,D). Observation of live *dlA^dx2/dx2^* embryos reveals that hair cells in the anterior and posterior maculae often spread together to form a contiguous lawn, in agreement with the pattern of *pax2.1* expression.

Fig. 1. Expression of *pax2.1* in the inner ear of wild-type and *dlA*[dx2/dx2] embryos. (A-C) Dorsolateral view of the otic vesicle at 24 h showing accumulation of *pax2.1* transcripts in a wild-type embryo (A), a moderately affected *dlA*[dx2/dx2] mutant (B) and a severely affected *dlA*[dx2/dx2] mutant (C). Cells lining the medial wall of the otic vesicle are heavily labeled, including small groups of cells in the developing sensory patches (arrows). In the *dlA*[dx2/dx2] mutants, increased numbers of labeled cells are evident in the sensory epithelia. (D,E) Dorsolateral view of the otic vesicle at 24 h showing immunofluorescent staining with two antibodies: one directed against acetylated tubulin and the other generated against mouse Pax2. Within the otic vesicle, anti-acetylated tubulin specifically labels the apical surfaces and kinocilia of hair cells (Haddon and Lewis, 1996; Riley et al., 1997). In both wild-type (D) and *dlA*[dx2/dx2] (E) embryos, hair cell nuclei show strong anti-Pax2 staining (arrows), and hair cells are overproduced in the *dlA*[dx2/dx2] mutant. (F,G) Lateral view of the nascent otic vesicle at 18.5 h showing immunofluorescent staining with anti-Pax2 antibody in a wild-type embryo (F) and a *noi*[tb21/tb21] (*pax2.1*) mutant (G). (H,I) Lateral view of the posterior trunk and tail region showing immunofluorescent staining with anti-Pax2. Nuclei are labeled in the developing pronephros (p) and in a subset of neurons in the spinal cord (sc). (J) Dorsolateral view of anterior hair cells in a *noi*[tb21/tb21] mutant at 24 h labeled with antibodies directed against acetylated tubulin and Pax2. Hair cell apices and kinocilia are strongly labeled with anti-acetylated tubulin (arrow), but nuclear Pax2 staining is no longer detectable. Because *noi*[tb21] reduces expression of *pax2.1* (Brand et al., 1996) but not *pax2.2* (Pfeffer et al., 1998), these data suggest that the Pax2 antibody used here preferentially recognizes pax2.1. (A-G,J) Anterior is to the left and dorsal is upward. (H,I) Anterior is to the right and dorsal is downward. Scale bar, 10 μm (J), 20 μm (D,E), 35 μm (A-C), 60 μm (F,G), and 115 μm (H,I).
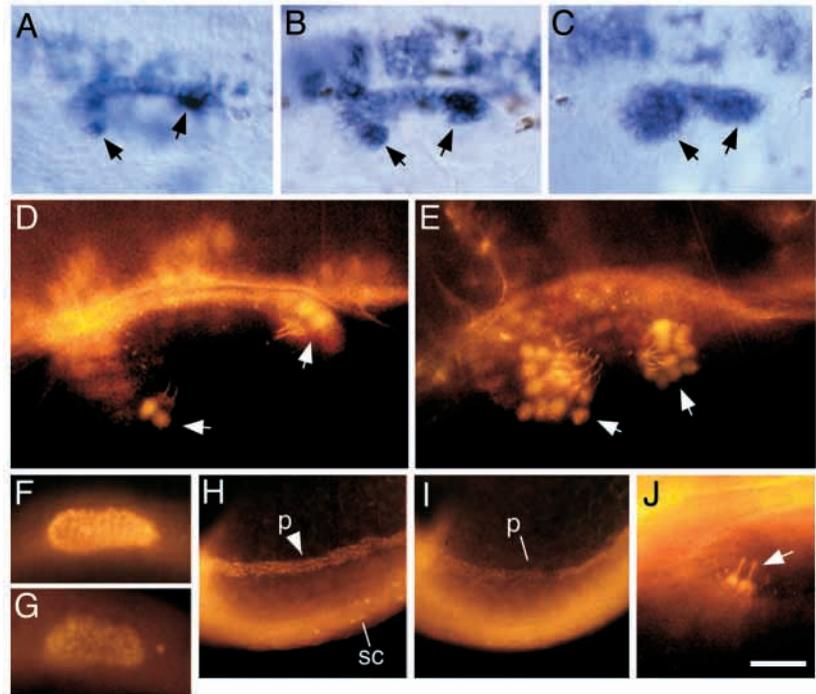
Otolith formation is usually delayed by several hours in *dlA*[dx2/dx2] embryos (not shown), probably reflecting a severe reduction in support cell function(s) that are normally required for deposition of otolith precursor materials (Riley and Grunwald, 1996; Riley et al., 1997). By 30 h, otoliths are usually present but are variable in number and morphology (Fig. 3D).

In severely affected *dlA*[dx2/dx2] embryos (Fig. 3A,C,D), the semicircular canals and cristae do not develop properly. However, the *dlA*[dx2] mutation is variable in its effects and permits some homozygotes to develop more normally. Analysis of moderately affected *dlA*[dx2/dx2] embryos revealed that, as with the maculae, cristae also develop with an excess of hair cells (Fig. 3E). Thus, the *dlA*[dx2] phenotype strongly supports the hypothesis that lateral inhibition mediated by *dlA* normally establishes the interspersed pattern of hair cells and support cells.

Fig. 2. Differentiation of hair cells in wild-type embryos. (A) Dorsolateral view of the otic vesicle at 30 h showing anti-Pax2 staining. The nuclei of presumptive hair cells stain intensely (arrows) whereas surrounding cells show lower staining levels. (B) Parasagittal section of a 30 h embryo stained in whole mount with anti-Pax2 and anti-acetylated tubulin antibodies. Hair cells in the utricular macula are marked by their strong nuclear Pax2 staining (arrow), as well as their stained kinocilia and associated otolith (o). Support cells show no detectable staining. (C) Dorsal view of the otic vesicle at 48 h showing anti-Pax2 staining in the utricular macula. The nuclei of hair cells stain intensely (arrow) and presumptive nascent hair cells (n) surrounding the macula show lower staining levels. (D) Longitudinal section of a 60 h embryo stained in whole mount with anti-Pax2 and anti-acetylated tubulin antibodies. In this slightly oblique dorsal view of the saccular macula, the kinocilia are not visible, but hair cells are clearly marked by their nuclear anti-Pax2 staining (arrow) and the close proximity of the otolith (o). Support cells are not labeled. (E) Lateral view of the otic vesicle at 60 h showing anti-Pax2 staining in the cristae (c). (F) Lateral view of posterior crista in a 60 h embryo stained with anti-Pax2 (red) and anti-acetylated tubulin (green). Hair cells (arrow) show nuclear Pax2 staining and ciliary acetylated tubulin staining. Support cells are not labeled. In all panels, anterior is to the right. (A,B,E,F) Dorsal is up; (C) medial is upward, and (D) medial is downward. Scale bar, 15 μm (F), 20 μm (A-D), or 65 μm (E).
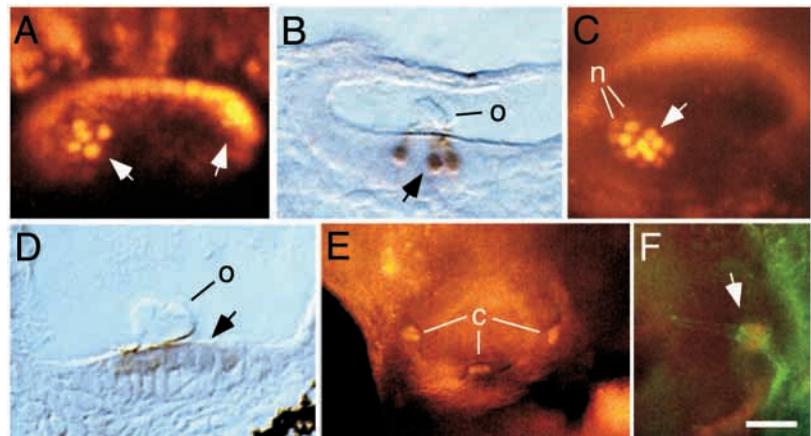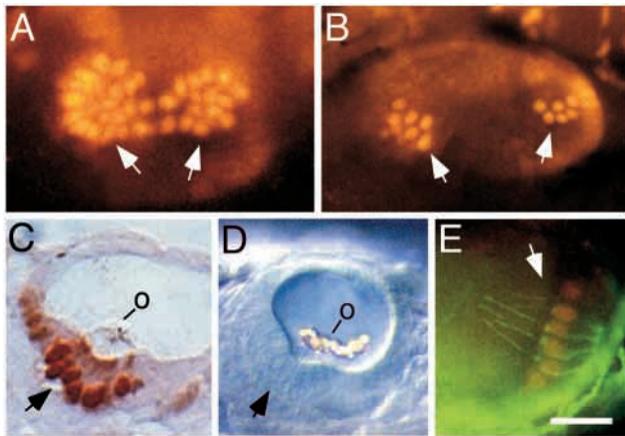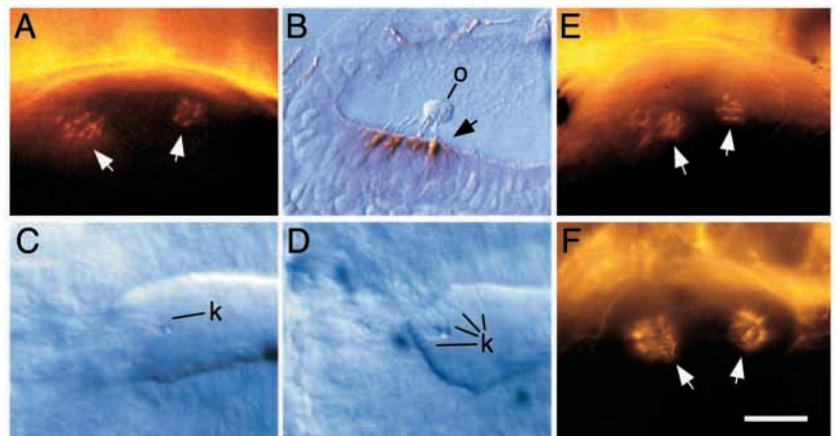
Fig. 3. Overproduction of hair cells in $dlA^{dx2/dx2}$ mutants.
(A) Dorsolateral view of the otic vesicle of a 30 h $dlA^{dx2/dx2}$ embryo stained with anti-Pax2 antibody. Hair cells stain intensely (arrows) and are produced in much greater numbers than normal.
(B) Dorsolateral view of the otic vesicle of a 30 h $dlA^{dx2}/T(msxB)^{b220}$ trans-heterozygote stained with anti-Pax2 antibody. Stained hair cells (arrows) are produced in excess, but to a lesser degree than in $dlA^{dx2/dx2}$ homozygotes. (C) Parasagittal section of a $dlA^{dx2/dx2}$ embryo stained in whole mount with anti-Pax2 and anti-acetylated tubulin antibodies. Large numbers of hair cells are labeled (arrow), but few support cells are evident. An otolith (o) is attached to the hair cell ciliary bundles. (D). Lateral view of the otic vesicle of a live $dlA^{dx2/dx2}$ embryo as seen under DIC optics. Numerous hair cells are evident (arrow) and a large malformed otolith (o) is distributed across the tips of the hair cell ciliary bundles. (E) Lateral view of the posterior crista of a 60 h $dlA^{dx2/dx2}$ embryo stained in with anti-Pax2 (red) and anti-acetylated tubulin (green) antibodies. Hair cells show nuclear Pax2 staining and are produced in greater than normal numbers. Anterior is to the right and dorsal is to the top. Scale bar, 15 µm (E), 20 µm (A-C), or 25 µm (D).

Hair cell differentiation in *no isthmus* mutants

Expression of *pax2.1* in hair cells suggested that *pax2.1* might play an essential role in hair cell differentiation. To address this
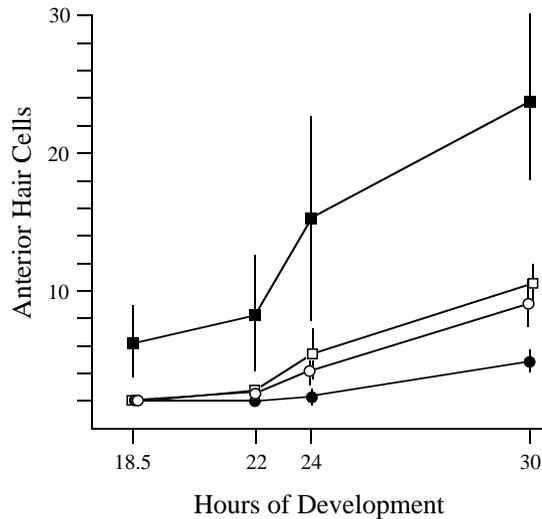
Table 1. Effects of various mutations on hair cell production at 30 hours

Genotype	Number of hair cells in maculae (mean ± s.e.m.)	Fold increase relative to wild type	Number of experiments	Total number of embryos
+/+	7.2±0.2	1.0	4	56
$dlA^{dx2/dx2}$	38.3±2.8	5.3	3	50
$dlA^{dx2/+}$	12.7±0.7	1.7	5	75
$dlA^{dx2}/T(msxB)^{b220}$	19.7±3.5	2.7	3	59
$T(msxB)^{b220/+}$ *	7.1±0.1	1.0	3	46
$noi^{tb21/tb21}$	13.2±0.1	1.8	4	64
$noi^{tb21/+}$ *	7.2±0.2	1.0	3	46
$dlA^{dx2/dx2}; noi^{tb21/tb21}$	17.2±0.5	2.4	3	36
$noi^{tb21/tb21}; T(msxB)^{b220/+}$ *	15.5±0.2	2.2	4	68
$mib^{ta52b/ta52b}$	71.0±3.8	9.9	2	15
$mib^{ta52b/+}$ *	7.3±0.2	1.0	2	26
$dlA^{dx2/dx2}; mib^{ta52b/ta52b}$ *	68.4±4.0	9.5	2	20
$mib^{ta52b/ta52b}; noi^{tb21/tb21}$	68.2±4.3	9.5	2	12

*These genotypes could not be directly identified but were inferred to make up a predictable fraction of their respective clutches based upon the genotypes of the parents. For analysis of $T(msxB)^{b220/+}$, $noi^{tb21/+}$ and $mib^{ta52b/+}$ embryos, heterozygous parents were outcrossed to wild-type partners and the resulting progeny were analyzed, half of which were expected to be heterozygous for the respective mutation. For analysis of $noi^{tb21/tb21}; T(msxB)^{b220/+}$ embryos, $T(msxB)^{b220/+}; noi^{tb21/+}$ double heterozygotes were crossed to $noi^{tb21/+}$ partners and $noi^{tb21/tb21}$ progeny were analyzed, half of which were expected to be $T(msxB)^{b220/+}$ heterozygotes. For analysis of $dlA^{dx2/dx2}; mib^{ta52b/ta52b}$ embryos, $dlA^{dx2/+}; mib^{ta52b/+}$ double heterozygotes were intercrossed and $mib^{ta52b/ta52b}$ progeny were analyzed, 25% of which were expected to be $dlA^{dx2/dx2}$ homozygotes.

All other genotypes were determined according to the criteria listed in Materials and Methods.

issue, we examined hair cell differentiation in $noi^{tb21/tb21}$ mutant embryos by staining with antibodies to detect both pax2.1 and acetylated tubulin. As seen in both whole-mounts and sections of stained specimens (Fig. 4A,B), numerous hair cells are produced in $noi^{tb21/tb21}$ embryos by 30 h, despite the absence of detectable pax2 protein. Indeed, $noi^{tb21/tb21}$ embryos display a weak neurogenic phenotype in the ear, typically producing nearly twice the normal number of hair cells by 30 h (Table 1).

Fig. 4. Genetic interactions between noi^{tb21}, dlA^{dx2} and mib^{ta52b}. (A) Dorsolateral view of the otic vesicle of a 30 h $noi^{tb21/tb21}$ embryo stained with anti-Pax2 and anti-acetylated tubulin antibodies. Nuclear staining is not detectable, but the apical surfaces and kinocilia of hair cells are strongly labeled (arrows). Twice the normal number of hair cells are evident.
(B) Parasagittal section of a $noi^{tb21/tb211}$ mutant stained in whole mount with anti-Pax2 and anti-acetylated tubulin antibodies. Nuclear pax2 staining is not detectable, but hair cells are clearly marked by acetylated tubulin staining (arrow) and the close association with the otolith (o). (C) Otic vesicle of a live $noi^{tb21/tb21}$ mutant viewed under DIC optics at 19 h. The kinocilia (k) of two tether cells, and attached otolith precursors, are seen at the anterior end of the otic vesicle. (D) Otic vesicle of a live $dlA^{dx2/dx2}$

mutant viewed under DIC optics at 19 h. The kinocilia (k) of supernumerary tether cells are evident. (E) Dorsolateral view of the otic vesicle of a 30 h $dlA^{dx2/dx2}; noi^{tb21/tb21}$ double mutant stained with anti-Pax2 and anti-acetylated tubulin antibodies. Hair cells, detected by staining of their kinocilia and apical surfaces (arrows), are produced in numbers that are comparable to $noi^{tb21/tb21}$ single mutants. (F) Dorsolateral view of the otic vesicle of a 30 h $mib^{ta52b.ta52b}; noi^{tb21/tb21}$ double mutant stained with anti-Pax2 and anti-acetylated tubulin antibodies. Hair cells (arrows) are produced in much greater numbers than in $noi^{tb21/tb21}$ single mutants. In all panels, anterior is to the right and dorsal is up. Scale bar, 10 µm (C,D), 15 µm (B), or 25 µm (A,E,F).

Fig. 5. Time course of hair cell formation in utricular maculae. Tether cells were visualized in live embryos at 18.5 and 21 h. At later stages of development, hair cells were visualized by fixing and staining embryos with anti-Pax2 and/or anti-acetylated tubulin antibodies. Utricular (anterior) maculae are easily visualized in live specimens and show faster rates of growth than saccular maculae in all genetic backgrounds. Each time point shows the mean and standard deviation of data pooled from three clutches of 10 or more embryos each. Symbols: (●) wild-type, (○) $noi^{tb21/tb21}$, (■) $dlA^{dx2/dx2}$ and (□) $dlA^{dx2/dx2}; noi^{tb21/tb21}$ embryos.

By comparison, $dlA^{dx2/dx2}$ embryos typically produce about a five-fold excess of hair cells by 30 h.

To better characterize the extent of hair cell hyperplasia, we determined the time course of hair cell production during the early stages of otic vesicle development in +/+, $dlA^{dx2/dx2}$ and $noi^{tb21/tb21}$ embryos. The first hair cells to differentiate in the otic vesicle are termed 'tether cells', which constitute a precocious cell type analogous to primary neurons. Although tether cells initially appear morphologically immature and fully span the epithelium, they nevertheless possess functional kinocilia that serve to localize otolith accretion over the developing maculae (Riley et al., 1997). In wild-type embryos, we invariably observe two tether cells in both anterior and posterior maculae at the onset of otic vesicle formation at 18.5 h (Riley et al., 1997). Tether cells eventually acquire a more typical hair cell morphology that is indistinguishable from that of later forming hair cells, which begin to accumulate after 24 h. By 30 h, the anterior macula normally possesses around five hair cells, which includes the two mature tether cells. In $noi^{tb21/tb21}$ embryos, the number of tether cells produced during early stages of otic vesicle development is normal (Fig. 4C) whereas later forming hair cells are produced in excess, yielding about twice the normal number of hair cells by 30 h (Figs 4A, 5; Table 1). In $dlA^{dx2/dx2}$ embryos, both tether cells (Fig. 4D) and later forming hair cells are produced in excess, with about a five-fold excess of hair cells becoming evident by 30 h (Fig. 5; Table 1). Thus, although they are not as severely affected as $dlA^{dx2/dx2}$ embryos, $noi^{tb21/tb21}$ mutants produce a significant excess of hair cells. These data suggest that $pax2.1$ is not essential for hair cell differentiation but that it may play a role in limiting the number of cells that differentiate as hair cells.

To examine this further, we generated $dlA^{dx2/dx2}; noi^{tb21/tb21}$ double mutants to determine whether the two mutations interact genetically. To our surprise, inner ear development in $dlA^{dx2/dx2}; noi^{tb21/tb21}$ double homozygotes is nearly identical to that of $noi^{tb21/tb21}$ homozygotes: double mutants initially produce a normal number of tether cells but produce just over twice the normal number of hair cells by 30 h (Figs 4E, 5; Table 1). Thus, noi^{tb21} strongly suppresses the dlA^{dx2} phenotype, suggesting that $pax2.1$ and dlA participate in the same developmental pathway.

Expression of *dlA* and *dlD* in developing hair cells

To better understand the effects of dlA^{dx2} and noi^{tb21} on hair cell development and lateral inhibition, we analyzed expression of dlA and dlD in the inner ear of wild-type and mutant embryos. dlA and dlD are initially expressed in hair cell precursors at the anterior and posterior ends of the otic placode by 14 h (Haddon et al., 1998a). Expression in tether cells is evident in the newly formed otic vesicle at 19 h in wild-type embryos and, as expected, this population of cells is overproduced in dx2 mutants (Fig. 6A,C,D,F). By 30 h of development, dlA and dlD are downregulated to very low or undetectable levels in mature hair cells. However, at the margin of each macula in wild-type embryos, we typically observe one or two cells that express these genes at relatively high levels (Fig. 7A,E). These cells, which fully span the epithelium, appear to be nascent hair cells undergoing early stages of differentiation (Haddon et al., 1998a). In $dlA^{dx2/dx2}$ embryos, nascent hair cells with high levels of dlA and dlD expression are produced in excess (Fig. 7C,G). These data provide further evidence that dlA^{dx2} disrupts lateral inhibition, thereby increasing the number of cells differentiating as hair cells.

In $noi^{tb21/tb21}$ embryos, the overall pattern of dlA and dlD expression is similar to that seen in wild-type embryos (Figs 6B,E, 7B,F). However, the level of expression in nascent hair cells in noi^{tb21} embryos is variably reduced compared to the wild type. Moreover, the number of nascent hair cells with detectable expression of dlA and dlD is not elevated in $noi^{tb21/tb21}$ embryos, even though they produce twice the normal number of hair cells. Similarly, $dlA^{dx2/dx2}; noi^{tb21/tb21}$ double mutants express dlA and dlD at lower levels, and in fewer cells, than do $dlA^{dx2/dx2}$ mutants (Fig. 7D,H). Together, these observations suggest that the noi^{tb21} mutation reduces the magnitude and/or duration of maximal dlA and dlD expression in nascent hair cells. Quantitative PCR analysis of whole embryo RNA confirms that $noi^{tb21/tb21}$ mutants show a 25% decrease in overall dlA mRNA levels compared to wild-type embryos (Fig. 8). Moreover, results of in situ hybridization experiments indicate that noi^{tb21} preferentially reduces dlA expression levels in tissues that also express $pax2.1$, especially the otic vesicle and lateral hindbrain (Fig. 7 and data not shown). Hence, the level of dlA expression in hair cells is likely to be reduced by considerably more than 25% in $noi^{tb21/tb21}$ mutants. Because the efficiency of Delta-Notch signaling is highly sensitive to changes in Delta protein levels, it is likely that the reduced expression of dlA and dlD observed in $noi^{tb21/tb21}$ embryos is sufficient to weaken signals required for lateral inhibition, thus providing an explanation for why these mutants produce supernumerary hair cells. Furthermore, reduced levels of transcription from the mutant dlA^{dx2} locus could also explain the ability of noi^{tb21} to suppress the dlA^{dx2}

phenotype. Since *dlA^{dx2}* encodes a dominant negative protein, reducing the level of the mutant protein would be expected to ameliorate its effects.

Altering *dlA* gene dosage affects hair cell production

If *noi^{tb21}* affects lateral inhibition in hair cells by reducing expression of *dlA* and *dlD*, then *T(msxB)^{b220}*, a deletion that removes the *dlA* locus (Fritz et al., 1996), should enhance the neurogenic effects of *noi^{tb21}* by further reducing *dlA* levels. Analysis of *T(msxB)^{b220/b220}* homozygotes is confounded by the phenotypic severity of the large *T(msxB)^{b220}* deletion. *T(msxB)^{b220/+}* heterozygotes, on the contrary, appear normal and produce a normal number of hair cells (Table 1). This indicates that there is sufficient redundancy in *delta* gene function to compensate for the loss of a single copy of *dlA*. Nevertheless, populations of embryos with equal numbers of *noi^{tb21/tb21}*; *T(msxB)^{b220/+}* double mutants and *noi^{tb21/tb21}* single mutants show a 20% increase in mean hair cell production compared to *noi^{tb21/tb21}* alone (Table 1). This increase is highly reproducible and statistically significant ($P<0.025$). Moreover, it probably underestimates the effect of *T(msxB)^{b220}* since non-*T(msxB)^{b220}* carriers cannot be identified and excluded from such populations. Thus, halving the level of *dlA* alone is not sufficient to disrupt lateral inhibition, but is sufficient to enhance the *noi^{tb21}* phenotype. This suggests that once Delta-Notch signaling drops below a critical threshold, quantitative changes in the efficiency of lateral inhibition are more easily observed such that haploinsufficiency of *dlA* enhances the neurogenic effects of *noi^{tb21}*.

Additional evidence that dosage of the wild-type and mutant alleles of *dlA* affects lateral inhibition of hair cells comes from analysis of interactions between *dlA^{dx2}* and *T(msxB)^{b220}*. Unlike *T(msxB)^{b220/+}* heterozygotes, *dlA^{dx2/+}* heterozygotes show a weak neurogenic phenotype, producing an average of 70% more hair cells than normal (Table 1). *dlA^{dx2}/T(msxB)^{b220}* *trans*-heterozygotes produce nearly three-fold more hair cells than normal (Fig. 3B; Table 1), a value that lies between those seen in *dlA^{dx2/dx2}* homozygotes and *dlA^{dx2/+}* heterozygotes. Thus, expressing two copies of the *dlA^{dx2}* allele causes a more complete disruption of lateral inhibition than does a single copy, and expressing one copy of *dlA^{dx2}* alone is more severe than co-expressing *dlA^{dx2}* along with the wild-type allele of *dlA*. These data are consistent with notion that *dlA^{dx2}* encodes an antimorphic protein that interferes with the function of wild-type *dlA*, as well as other *delta* homologs, and that lateral inhibition is a sensitive function of total levels of Delta-Notch signaling.

mib^{ta52b} is epistatic to *dlA^{dx2}* and *noi^{tb21}*

Because *mib* is the only other neurogenic mutation yet described in zebrafish, we wished to compare the effects of *mib^{ta52b}* to those of *dlA^{dx2}* and *noi^{tb21}*. The gene affected by the *mib* mutation has not yet been identified, but results of several studies strongly suggest that *mib* disrupts Delta-Notch signaling and lateral inhibition (Jiang et al., 1996; Schier et al., 1996; Haddon et al., 1998a). The *mib^{ta52b}* phenotype is similar to that of *dlA^{dx2}*, although *mib^{ta52b}* is more severe and affects a wider range of tissues. In the developing inner ear, *mib^{ta52b/ta52b}* mutants produce a 10-fold excess of *pax2.1*-

expressing hair cells by 30 h (Table 1). *mib^{ta52b/ta52b}*; *noi^{tb21/tb21}* double mutants produced the same number of hair cells as *mib^{ta52b.ta52b}* single mutants (Fig. 4F; Table 1). Thus, *mib^{ta52b}* is epistatic to *noi^{tb21}*, suggesting that *mib^{ta52b}* is unaffected by changing levels of *delta* gene expression. Furthermore, *mib^{ta52b}* also appears to be epistatic to *dlA^{dx2}*: Intercrosses between *dlA^{dx2/+}*; *mib^{ta52b/+}* double heterozygotes yield the expected ratio of *mib^{ta52b/ta52b}* progeny but too few *dlA^{dx2/dx2}* progeny. For example, among progeny pooled from three such intercrosses, 112/411 (27%) appeared as *mib^{ta52b/ta52b}* homozyotes, but only 70/411 (17%) showed the *dlA^{dx2/dx2}* phenotype. We infer that 1/4 of *mib^{ta52b/ta52b}* progeny are also homozygous for *dlA^{dx2}*, but that the more severe *mib^{ta52b/ta52b}* phenotype masks the presence of *dlA^{dx2}*. Accordingly, we observed no difference in hair cell production in populations containing presumptive *dlA^{dx2/dx2}*; *mib^{ta52b/ta52b}* double mutants compared to *mib^{ta52b/ta52b}* single mutants (Table 1). Together, these data could indicate that the *mib^{ta52b}* mutation blocks reception of Delta signals.

DISCUSSION

### *pax2.1* and *dlA* regulate patterning of the otic sensory epithelium

In this study, we have shown that *dlA* and *pax2.1* interact to regulate the initial differentiation and diversification of hair cells and support cells within the otic sensory epithelium. *pax2.1* is initially expressed in preotic cells 2-3 hours prior to formation of the otic placode, but its expression does not become regionally restricted within this domain until much later when the otic vesicle forms (Krauss et al., 1991). In contrast, *dlA*, *dlB* and *dlD* are expressed in the nascent otic placode in regions that later give rise to the sensory epithelia, constituting one of the earliest events yet reported for initial differentiation of the sensory epithelium (Haddon et al., 1998a). The developmental signals required for localized induction of the sensory epithelia have not been identified, but several studies suggest that signals from cephalic mesendoderm are involved. In zebrafish mutants lacking cephalic mesendoderm, induction of the otic placode is delayed, as revealed by belated expression of *pax2.1*, and the sensory epithelia are poorly formed (Mendonsa and Riley, 1999). In chick embryos, explanting otic placodes without surrounding periotic mesenchyme results in formation of vesicles with deranged sensory epithelia (Noden and Van de Water, 1986; Swanson et al., 1990). However, in all cases reported, local arrangements of support cells and hair cells are relatively normal. These data suggest that signals from surrounding mesendoderm are required for normal positioning of the sensory epithelia within the placode and vesicle, but that endogenous cues generate the interspersed arrangement of hair cells and support cells. Delta-Notch signaling appears to be the principle mechanism for controlling the latter function (Adam et al., 1998; Haddon et al., 1998a; this report).

In other species, induction of neural potential and subsequent *delta* gene expression require prior expression of proneural genes, including homologs of *atonal* or members of the *achete-scute complex* in *Drosophila* (Campos-Ortega, 1994; Artavanis-Tsakonas et al., 1995; Lewis, 1996; Bermingham, 1999). The proneural genes encode bHLH

Fig. 6. Expression of *dlA* and *dlD* in tether cells in the anlage of the maculae. Dorsal views of nascent otic vesicles at 19 h showing expression of *dlA* (A-C) or *dlD* (D-F) in tether cells (arrows). Wild-type embryos (A,D) and *noi*$^{tb21/tb21}$ mutants (B, E) show expression in pairs of tether cells in the anteromedial and posteromedial regions of the otic vesicle. In *dlA*$^{dx2/dx2}$ mutants (C,F), *delta*-expressing tether cells are produced in excess. Scale bar, 20 μm.
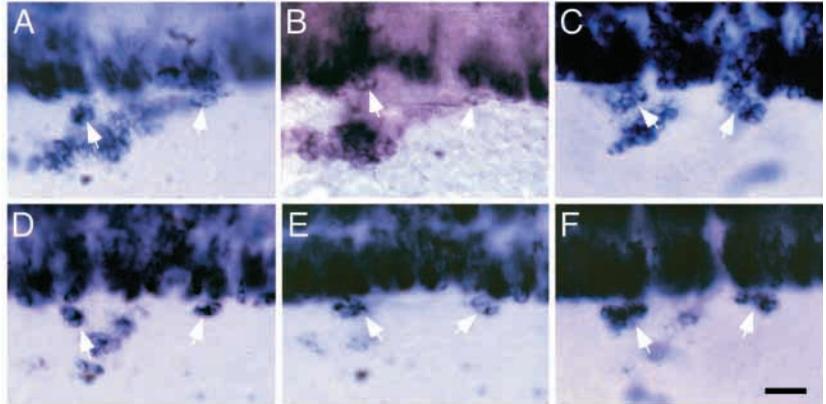
Fig. 7. Expression of *dlA* and *dlD* in hair cells in anterior maculae. Lateral views of utricular maculae at 30 h showing expression of *dlA* (A-D) or *dlD* (E-H) in nascent hair cells (arrows). Wild-type embryos (A,E) usually show only one or two labeled cells at this time. *noi*$^{tb21/tb21}$ mutants (B,F) show a normal number of stained cells, but expression levels are usually lower than normal. *dlA*$^{dx2/dx2}$ mutants (C,G) show supernumerary nascent hair cells with intense labeling, whereas *dlA*$^{dx2/dx2}$; *noi*$^{tb21/tb21}$ double mutants (D,H) show near normal numbers of nascent hair cells with reduced labeling. In all panels, anterior is to the right and dorsal is up. Scale bar, 15 μm.
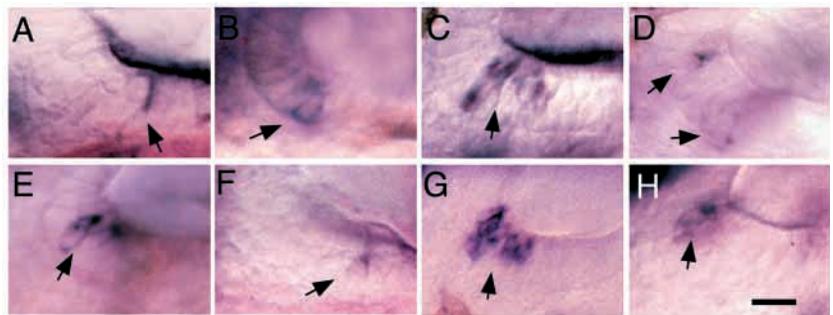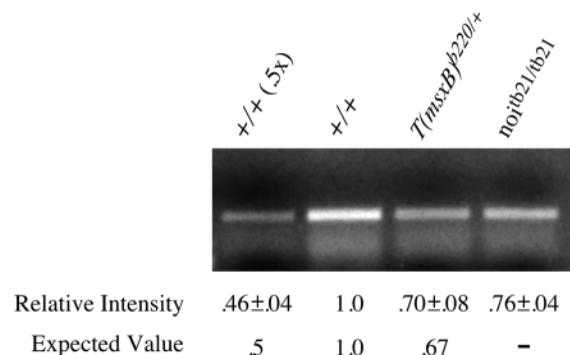

transcription factors that stimulate transcription of *delta* genes. Presumably, one or more proneural genes also regulate *delta* gene expression in the zebrafish inner ear. Although such proneural genes have not yet been identified, it is likely that they are expressed quite early in otic development, possibly in response to the same signals that induce expression of *pax2.1* in the preotic placode.

Fig. 8. Effect of *noi*^{tb21} on accumulation of *dlA* mRNA. RT-PCR was performed on total RNA extracted from pools of 40 +/+, *noi*$^{tb21/tb21}$, or *T(msxB)*$^{b220/+}$ embryos at 24 h. Equal volumes of the PCR reaction products were run out on a 1% agarose gel, stained with ethidium bromide and analyzed using a digital imaging system (Kodak EDAS-120). Fluorescence intensities are expressed as relative values with wild-type levels set at 1.0. Intensity data show the means and standard deviations of two independent RNA extractions, each subjected to RT-PCR analysis twice (4 experiments each). Two controls were performed in each experiment: First, to ensure that PCR amplification and quantitation remained in the linear range, a half aliquot of cDNA produced from +/+ RNA was PCR amplified and analyzed in parallel with a full aliquot of +/+ cDNA template. Second, to establish that the RT-PCR protocol used here accurately detects known changes in gene dosage, RNA was extracted from phenotypically normal embryos derived from an intercross between *T(msxB)*$^{b220/+}$ heterozygotes. Since 2/3 of such embryos are expected to be heterozygous, effective gene dosage should be 2/3 of the wild-type level. Both controls gave relative intensity levels that were statistically indistinguishable from expected values. RT-PCR analysis of RNA derived from *noi*$^{tb21/tb21}$ embryos showed that *noi*^{tb21} reduces *dlA* mRNA levels by roughly 25%. Similar results were obtained from extracts of 30 h embryos (not shown). Bands show PCR reaction products of 377 base pairs.

Possible mechanisms of *pax2.1* function

Although *pax2.1* expression precedes *delta* gene expression in developing hair cells, and disruption of *pax2.1* perturbs *delta* gene expression (Fig. 7), the function of *pax2.1* is not strictly analogous to that of a proneural gene. Expression of proneural genes is typically extinguished in neural cells as they begin to differentiate (Campos-Ortega, 1994; Lewis, 1996), whereas *pax2.1* is retained in hair cells following differentiation. Furthermore, the *noi* mutant phenotype indicates that *pax2.1* is not required for induction of the otic placode or the sensory epithelia, nor is it required for induction of *delta* gene expression. Instead, *pax2.1* is only required for optimal expression of *delta* genes in nascent hair cells. Expression levels of *dlA* and *dlD* are often reduced in nascent hair cells in *noi*$^{tb21/tb21}$ mutants, and the number of *delta*-expressing cells is lower than expected based on the number of mature hair cells that eventually form. These data suggest that, in *noi*$^{tb21/tb21}$

	+/+ (5x)	+/+	*T(msxB)*$^{b220/+}$	*noi*$^{tb21/tb21}$
Relative Intensity	.46±.04	1.0	.70±.08	.76±.04
Expected Value	.5	1.0	.67	–

mutants, maximal *delta* expression in differentiating hair cells is either delayed or prematurely attenuated. This misregulation is probably sufficient to weaken signals required for lateral inhibition, providing an explanation for why $noi^{tb21/tb21}$ mutants produce supernumerary hair cells. Reducing expression from the *dlA* locus also explains the ability of noi^{tb21} to suppress the phenotype of dlA^{dx2}, which encodes a dominant-negative protein. Indeed, halving the dose of dlA^{dx2} by generating *trans*-heterozygotes carrying a single copy each of dlA^{dx2} and $T(msxB)^{b220}$ (a deletion that removes the *dlA* locus) also partially suppresses dlA^{dx2}. In contrast, halving the dose of wild-type *dlA* by generating $T(msxB)^{b220/+}$ heterozygotes enhances the neurogenic effects of noi^{tb21}.

It is not yet clear how *pax2.1* affects *delta* gene expression. *pax2.1* could augment the actions of other transcription factors that are required for expression of *delta* genes. Alternatively, *pax2.1* could inhibit transcription of Notch-activated genes in nascent hair cells, making them insensitive to the effects of Delta signals from other cells. Because Notch activity typically inhibits *delta* expression in the receiving cell (Campos-Ortega, 1994; Artavanis-Tsakonas et al., 1995; Lewis, 1996), *pax2.1*-mediated inhibition of N signal transduction would tend to intensify and prolong *delta* gene expression in nascent hair cells. Thus, *pax2.1* could help to induce or amplify initial biases in Delta-Notch signaling associated with lateral inhibition. Finally, it is possible that *pax2.1* plays a more general role that only indirectly affects Delta-Notch signaling. Although *pax2.1* is not required for hair cell differentiation per se, it may regulate the sequence or duration of early events in the differentiation process. In this case, disruption of *pax2.1* could prematurely activate a relatively advanced phase of hair cell differentiation during which *delta* genes are normally downregulated. Analysis of *delta* promoter sequences and identification of additional markers of hair cell and support cell differentiation will help to resolve these issues.

It is possible that a relationship between *pax* function and Delta-Notch signaling has been conserved between invertebrates and vertebrates. A *pax2* homolog was recently identified in *Drosophila*, and two previously described mutations, *sparkling* and *shaven*, were found to disrupt distinct promoter elements that normally control regional expression of *pax2* (Fu and Noll, 1997; Fu et al., 1998). *sparkling* mutants develop with a rough eye phenotype resulting from defects in formation of cone and pigments cells. *shaven* mutants develop with a deficiency of sensory bristles due to a defect in the formation of shaft cells. Similar phenotypes are caused by mutations that alter Delta-Notch signaling, and genetic studies confirm that *pax2* and *Delta-Notch* cooperate to regulate differentiation of shaft cells in *Drosophila* (Kavaler et al., 1999). In *C. elegans*, *eg-l38* encodes a *pax2/5/8* homolog and mutants display defects in development of ventral uterine cells (Chamberlin et al., 1997). Disruption of *lin-12*, a *notch* homolog, perturbs development of the same cell population (Newman et al., 1995), suggesting that, here too, *pax* function might cooperate with lateral inhibition during normal development.

It is also possible that *Pax2* plays a similar role in mouse. Mouse *Pax2* is expressed in the developing inner ear and mice homozygous for a *Pax2* null mutation fail to produce a functional cochlea (Torres et al., 1996). Neurogenic defects were not reported in *Pax2* mutant mice, but such defects may have been relatively subtle, as we have observed in $noi^{tb21/tb21}$ mutants.

Other genes involved in lateral inhibition

In contrast to its effects on dlA^{dx2}, noi^{tb21} does not suppress the neurogenic effects of mib^{ta52b}. The gene affected by the mib^{ta52b} mutation has not yet been identified, but it seems likely that it affects some aspect of *notch* function or downstream signal transduction. The mib^{ta52b} phenotype is more severe and penetrant than that of dlA^{dx2}, as would be expected if mib^{ta52b} were to block reception of all Delta signals. This would also explain why mib^{ta52b} is epistatic to both dlA^{dx2} and noi^{tb21} (Table 1). Identification of the *mib* gene will greatly aid in our understanding of Delta-Notch signaling pathways in zebrafish, and genetic screens for second site modifiers of dlA^{dx2} and mib^{ta52b} could identify additional elements in the signaling pathway.

REFERENCES

Adam, J., Myat, A., Le Roux, I., Eddison, M., Henrique, D., Ish-horowicz, D. and Lewis, J. (1998). Cell fate choices and the expression of *Notch*, *Delta*, and *Serrate* homologues in the chick inner ear: parallels with *Drosophila* sense-organ development. *Development* **125**, 4645-4654.

Anniko, M. (1983). Embryonic development of vestibular sense organs and their innervation. In *Development of Auditory and Vestibular Systems* (ed. R. Romand), pp. 375-423. New York: Academic Press.

Appel, B. and Eisen, J. S. (1998). Regulation of neuronal specification in the zebrafish spinal cord by *Delta* function. *Development* **125**, 371-380.

Appel, B., Fritz, A., Westerfield, M., Grunwald, D. J., Eisen, J. S. and Riley, B. B. (1998). *Delta*-mediated specification of midline cell fates in zebrafish embryos. *Current Biology* **9**, 247-256.

Artavanis-Tsakonas, S., Matsuna, K. and Fortini, M. E. (1995). *Notch* signalling. *Science* **268**, 225-232.

Bermingham, N. A., Hassan, B. A., Price, S. D., Vollrath, M. A, Ben-Arie, N., Eatock, R. A., Bellen, H. J., Lysakowski, A. and Zoghbi, H. Y. (1999). *Math1*: An essential gene for the generation of inner ear hair cells. *Science* **284**, 1837-1841.

Brand, M., Heisenberg, C. P., Jiang, Y. J., Beuchle, D., Lun, K., Furutani-Seiki, M., Granato, M., Haffter, P., Hammerschmidt, M., Kane, D. A., Kelsh, R. N., Mullins, M. C., Odenthal, J., van Eeden, F. J. M. and Nüsslein-Volhard C. (1996). Mutations in zebrafish genes affecting the formation of the boundary between midbrain and hindbrain. *Development* **123**, 179-90.

Campos-Ortega, J. A. (1994). Cellular interactions in the developing nervous system of *Drosophila*. *Cell* **77**, 969-975.

Chamberlin, H. M., Palmer, R. E., Newman, A. P., Sternberg, P. W., Baillie, D. L. and Thomas, J. H. (1997). The *Pax* gene *egl-38* mediates developmental patterning in *Caenorhabditis elegans*. *Development* **124**, 3919-3928.

Chisaka, O., Musci, T. S. and Capecchi, M. R. (1992). Development defects of the ear, cranial nerves and hindbrain resulting from targeted disruption of the mouse homeobox gene *Hox-1.6*. *Nature* **355**, 516-520.

Chitnis, A., Henrique, D., Lewins, J., Ish Horowicz, D. and Kintner, C. (1995). Primary neurogenesis in *Xenopus* embryos regulated by a homologue of the *Drosophila* neurogenic gene *Delta*. *Nature* **375**, 761-766.

Cordes, S. P. and Barsh, G. S. (1994). The mouse segmentation gene *kr* encodes a novel basic domain-leucine zipper transcription factor. *Cell* **79**, 1025-1034.**

Corwin, J. T. and Warchol, M. E. (1991). Auditory hair cells: structure, function, development, and regeneration. *Ann. Rev. Neurosci*. **14**, 301-333.

de la Pompa, J. L., Wakeham, A., Correia, K. M., Samper, E., Brown, S., Aguilera, R. J., Nakano, T., Honjo, T., Mak, T. W., Rossant, J. and Conlon, R. A. (1997). Conservation of the *Notch* signalling pathway in mammalian neurogenesis. *Development* **124**, 1139-1148.

Epstein, D. J., Vekemans, M. and Gros, P. (1991). *splotch (sp2H)*, a mutation affecting development of the mouse neural tube, shows a deletion within the paired homeodomain of *Pax-3*. *Cell* **67**, 767-774.

Erkman, L., McEvilly, R. J., Luo, L., Ryan, A. K., Hooshmand, F., O'Connell, S. M., Keithley, E. M., Rapaport, D. H., Ryan, A. F. and Rosenfeld, M. G. (1996). Role of transcription factors *Brn-3.1* and *Brn-3.2* in auditory and visual system development. *Nature* **381**, 603-606.

Fritz, A., Rozowski, M., Walker, C. and Westerfield, M. (1996). Identification of selected gamma-ray induced deficiencies in zebrafish using multiplex polymerase chain reaction. *Genetics* **144**, 1735-1745.

Fu, W. and Noll, M. (1997). The *Pax2* homolog *sparkling* is required for development of cone and pigment cells in the *Drosophila* eye. *Genes Dev.* **11**, 2066-2078.

Fu, W., Duan, H., Frei, E. and Noll, M. (1998). *shaven* and *sparkling* are mutations in separate enhancers of the *Drosophila Pax2* homolog. *Development* **125**, 2943-2950.

Haddon, C. and Lewis, J. (1996). Early ear development in the embryo of the zebrafish, *Danio rerio*. *J. Comp. Neurol.* **365** 113-128.

Haddon, C., Jiang, Y.-L., Smithers, L. and Lewis, J. (1998a). *Delta-Notch* signalling and the patterning of sensory cell differentiation in the zebrafish ear: evidence from the *mind bomb* mutant. *Development* **125**, 4637-4644.

Haddon, C., Smithers, L., Schneider-Maunoury, S., Coche, T., Henrique, D. and Lewis, J. (1998b). Multiple delta genes and lateral inhibition in zebrafish primary neurogenesis. *Development* **125**, 359-370.

Hadrys, T., Braun, T., Rinkwitz-Brandt, S., Arnold, H.-H. and Bober, E. (1998). *Nkx5.1* controls semicircular canal formation in the mouse inner ear. *Development* **125**, 33-39.

Jiang, Y.-L., Brand, M., Heisenberg, C.-P., Beuchle, D., Furutani-Seiki, M., Kelsh, R. N., Warga, R. M., Granato, M., Haffter, P., Hammerschmidt, M., Kane, D. A., Mullins, M. C., Odenthal, J., van Eeden, F. J. M. and Nüsslein-Volhard, C. (1996). Mutations affecting neurogenesis and brain morphology in the zebrafish. *Development* **123**, 205-216.

Kavaler, J., Fu, W., Duan, H., Noll, M. and Posakony, J. W. (1999). An essential role for the *Drosophila* Pax2 homolog in the differentiation of adult sensory organs. *Development* **126**, 2261-2272.

Krauss, S., Johansen, T., Korzh, V. and Fjose, A. (1991). Expression of the zebrafish paired box gene *pax[zf-b]* during early neurogenesis. *Development* **113**, 1193-1206.

Lewis, E. R., Leverenz, E. L. and Bialek, W. S. (1985). *The Vertebrate Inner Ear*. Boca Raton, FL: CRC Press.

Lewis, J. (1996). Neurogenic genes and vertebrate neurogenesis. *Cur. Opinion Neurobiol.* **6**, 3-10.

Lufkin, T., Dierich, A., LeMeur, M., Mark, M. and Chambon, P. (1991). Disruption of the *Hox 1.6* homeobox gene results in defects in a region corresponding to its rostral domain of expression. *Cell* **66**, 1105-1119.

Lun, K. and Brand, M. (1998). A series of *no isthmus (noi)* alleles of the zebrafish *pax2.1* gene reveals multiple signaling events in development of the midbrain-hindbrain boundary. *Development* **125**, 3049-3002.

Mansour, S. L., Goddard, J. M. and Capecchi, M. R. (1993). Mice homozygous for a targeted disruption of the proto-oncogene *int-2* have developmental defects in the tail and inner ear. *Development* **117**, 13-28.

Mendonsa, E. S. and Riley, B. B. (1999). Genetic analysis of tissue-interactions required for otic placode induction in the zebrafish. *Dev. Biol.* **206**, 100-112.

Moens, C. B., Cordes, S. P., Giorgianni, M. W., Barsh, G. S. and Kimmel, C. B. (1998). Equivalence in the genetic control of hindbrain segmentation in fish and mouse. *Development* **125**, 381-391.

Newman, A. P., White, J. G. and Sternberg, P. W. (1995). The *Caenorhabditis elegans lin-12* gene mediates induction of ventral uterine specialization by the anchor cell. *Development* **121**, 263-271.

Noden, D. M. and Van de Water, T. R. (1986). The developing ear: Tissue origins and interactions. In *The Biology of Change in Otolaryngology* pp 15-46. Amsterdam: Elsevier Science Publishers.

Pfeffer, P. L., Gerster, T., Lun, K., Brand, M. and Busslinger, M. (1998). Characterization of three novel members of the zebrafish *Pax2/5/8* family: dependency of *Pax5* and *Pax8* on the *Pax2.1* (*noi*) function. *Development* **125**, 3063-3074.

Presson, J. C., Lanford, P. J. and Popper, A. N. (1996). Hair cell precursors are ultrastructurally indistinguishable from mature support cells in the ear of a postembryonic fish. *Hearing Res.* **100**, 10-11.

Riley, B. B. and Grunwald, D. J. (1996). A mutation in zebrafish affecting a localized cellular function required for normal ear development. *Dev. Biol.* **179**, 427-435.

Riley, B. B., Zhu, C., Janetopoulos, C. and Aufderheide, K. J. (1997). A critical period of ear development controlled by distinct populations of ciliated cells in the zebrafish. *Dev. Biol.* **191**, 191-201.

Schier, A. F., Neuhauss, S. C., Harvey, M., Malicki, J., Solnica-Krezel, L., Stainier, D. Y., Zwartkruis, F., Abdelilah, S., Stemple, D. L., Rangini, Z., Yang, H. and Driever, W. (1996). Mutations affecting the development of the embryonic zebrafish brain. *Development* **123**, 165-178.

Self, T., Mahony, M., Fleming, J. Walsh, J., Brown, S. D. M. and Steel, K. P. (1998). *Shaker-1* mutations reveal roles for *myosin VIIA* in both development and function of cochlear hair cells. *Development* **125**, 557-566.

Stachel, S. E., Grunwald, D. J. and Myers, P. Z. (1993). Lithium perturbations and *goosecoid* expression identify a dorsal specification pathway in the pregastrula zebrafish. *Development* **117**, 1261-1274.

Swanson, G. J., Howard, M. and Lewis, J. (1990). Epithelial autonomy in the development of the inner ear of a bird embryo. *Dev. Biol.* **137**, 243-257.

Torres, M., Gomez-Pardo, E. and Gruss, P. (1996). *Pax2* contributes to inner ear patterning and optic nerve trajectory. *Development* **122**, 3381-3391.

Wang, W., Van De Water, T. and Lufkin, T. (1998). Inner ear and maternal reproductive defects in mice lacking the *Hmx3* homeobox gene. *Development* **125**, 621-634.

Whitfield, T. T; Granato, M., van Eeden, F. J. M., Schach, U., Brand, M., Furutani-Seiki, M., Haffter, P., Hammerschmidt, M., Heisenberg, C.-P., Jiang, Y.-J., Kane, D. A., Kelsh, R. N., Mullins, M. C., Odenthal, J. and Nüsslein-Volhard, C. (1996). Mutations affecting development of the zebrafish inner ear and lateral line. *Development* **123**, 241-254.

Xiang, M., Gan, L., Li, D., Chen, Z.-Y., Zhou, L., O'Malley, B. W., Jr., Klein, W. and Nathans, J. (1997). Essential role of POU-domain factor *Brn-3c* in auditory and vestibular hair cell development. *Proc. Natl. Acad. Sci. USA* **94**, 9445-9450.